



## Research paper

Influence of methanol when used as a water-miscible carrier of pharmaceuticals in TiO<sub>2</sub> photocatalytic degradation experiments

Maricor J. Arlos<sup>a,\*</sup>, Robert Liang<sup>b,c</sup>, Lena C.M. Li Chun Fong<sup>b</sup>, Norman Y. Zhou<sup>b,c</sup>, Carol J. Ptacek<sup>d</sup>, Susan A. Andrews<sup>e</sup>, Mark R. Servos<sup>a</sup>

<sup>a</sup> Department of Biology, University of Waterloo, Waterloo, Ontario N2L 3G1, Canada

<sup>b</sup> Centre for Advanced Materials Joining, Department of Mechanical and Mechatronics Engineering, University of Waterloo, Waterloo, Ontario N2L 3G1, Canada

<sup>c</sup> Waterloo Institute for Nanotechnology, University of Waterloo, Waterloo, Ontario N2L 3G1, Canada

<sup>d</sup> Department of Earth and Environmental Sciences, University of Waterloo, Waterloo, Ontario N2L 3G1, Canada

<sup>e</sup> Department of Civil Engineering, University of Toronto, Toronto, Ontario M5S 1A4, Canada

## ARTICLE INFO

## Keywords:

Titanium dioxide  
Methanol  
Pharmaceuticals  
Carrier solvent  
Scavenger  
Radicals

## ABSTRACT

Research on the use of titanium dioxide (TiO<sub>2</sub>) for water treatment has expanded to include the degradation of pharmaceuticals and personal care products (PPCPs). PPCPs are typically introduced in aqueous solutions during TiO<sub>2</sub> photocatalysis experiments using a water-miscible carrier solvent (e.g. methanol) to improve their solubility; however, carrier solvents may be detrimental to photocatalysis due to their scavenging effect. Although it is advisable to maintain the solvent at low concentrations, the influence of elevated concentrations of methanol or other solvents on photocatalysis has not been carefully explored. In this study, we examined the impacts of different methanol concentrations (0–0.2% v/v) on photocatalysis using P25 (commercial TiO<sub>2</sub>) and TiO<sub>2</sub> nanomaterial synthesized via thermal and chemical oxidation (TCO). Scavenging of hydroxyl radicals by methanol was evident for both P25 and TCO but the effect was more prominent on TCO. Also, the photodegradation of some compounds using P25 were enhanced at low levels of methanol. Overall, this study highlights that trace amounts of methanol used as a carrier solvent can affect photocatalysis, especially in TiO<sub>2</sub> nanomaterials with low reactivity. This should be considered carefully in future experiments so that the results are not biased by the introduction of carrier solvents.

## 1. Introduction

Studies on the use of titanium dioxide (TiO<sub>2</sub>) for environmental applications has grown rapidly since the discovery of its photocatalytic potential over four decades ago [1]. Among the semiconductors that can initiate photocatalytic processes, TiO<sub>2</sub> is the most widely used material due to its relatively higher activity, non-toxic effects, inert qualities, resistance to corrosion, and low associated costs [2]. The use of TiO<sub>2</sub> for a variety of industrial applications began in the 1990s, mainly as a paint additive and glass coating because of its self-cleaning and anti-fogging functions [3]. With advances in nanoscience and nanotechnology, alternative synthesis methods and improvement in TiO<sub>2</sub> structural properties continue to progress. Alongside this development is the pressing need for advanced, low-cost, and efficient water treatment technologies to address the declining clean water sources worldwide [4]. In addition, long-term droughts and increased water demands have motivated the development of new water reuse, recycling, and reclamation strategies (i.e., indirect potable or non-potable reuse

systems) that stress the need for robust treatment technologies to handle a diversity of contaminants emanating from unconventional water sources [5]. The ubiquity of the so-called emerging contaminants of concern in source waters, primarily pharmaceuticals and personal care products (PPCPs), has been a subject of water research for a number of years due to their potential risks to aquatic and human health [6]. These combined challenges have encouraged several research and development studies that highlighted the potential use of TiO<sub>2</sub> photocatalysis for water treatment applications.

Numerous studies have suggested the use of TiO<sub>2</sub> photocatalysis in the effective degradation of PPCPs in water [7–9]. Much of the current work has also employed methanol as a carrier solvent when conducting TiO<sub>2</sub> photocatalytic degradation experiments on PPCPs (Table 1). This practice facilitates the introduction of the compounds into aqueous matrices, as some are poorly soluble in water. However, the presence of methanol can be detrimental to PPCP removal due to its ability to scavenge the electron holes [10] and/or the hydroxyl radicals [11] produced during photocatalysis. When an organic compound is present,

\* Corresponding author.

E-mail address: [mjarlos@uwaterloo.ca](mailto:mjarlos@uwaterloo.ca) (M.J. Arlos).

**Table 1**

Selected studies that employed carrier solvents during experimental investigations of photocatalytic decomposition of pharmaceuticals.

Carrier Solvent	No. of compounds	Carrier solvent concentration (v/v)	Reference
Methanol	15	0.004% <sup>a</sup>	[9]
Methanol	1	0.17%	[17]
Acetonitrile	4	0.953% <sup>a</sup>	[33]
Methanol	15	0.004% <sup>a</sup>	[8]
Methanol	2	0.5% <sup>b</sup>	[34]
Methanol	1	0.01%	[35]
Methanol	3	N/A	[36]
Methanol	33	0.4% <sup>a</sup>	[37]
Methanol	15	0.004% <sup>a</sup>	[38]
Methanol	2	0.1%	[39]
Ethanol	2	0.075% <sup>a</sup>	[40]
Methanol	14	0.002%	[16]
Methanol	5	0.002%	[23]

<sup>a</sup> Calculated based on the data provided in the study.

<sup>b</sup> Calculated based on the highest concentration of the target chemical in the mixture (~5 mg/L). N/A = not available nor cannot be calculated from the information provided.

its degradation via TiO<sub>2</sub> photocatalysis occurs in two main pathways: (1) reactions via singlet electron transfer (SET) (i.e. hole-mediated and electron-donating processes); or, (2) reactions with hydroxyl radicals and other generated reactive oxygen species [12]. Methanol degradation is typically initiated by SET chemistry (i.e. hole-mediated) [12,13] and, in fact, it has been used as an efficient hole scavenger in photocatalytic experiments [12]. However, there is still a mixed interpretation of the degradation pathway of alcohols as studies have utilized methanol as a hydroxyl radical scavenger rather than a hole scavenger [11,14]. This practice was derived from experiments that did not observe the presence of ketone- and aldehyde-type intermediates which are indicator compounds for SET reactions [12]. Regardless of the mechanism, only a few studies have discussed the effects of the carrier solvent on their photocatalysis experiments [15–19]. Although methanol and other carrier solvents are typically maintained at low concentrations from 0.002% to 0.5% v/v (Table 1), it is still important to assess the scavenging effects of these low concentrations of solvents when determining the overall efficiency of TiO<sub>2</sub> photocatalysis in degrading pharmaceuticals or other similar chemicals.

In this study, we explored the influence of low levels of methanol additions (0%, 0.002%, 0.02% and 0.2% v/v) on photocatalytic degradation of 15 target compounds typically discharged in wastewater streams [20,21]. The photocatalysis of these representative contaminants using commercially available TiO<sub>2</sub> nanopowder (P25) was compared to a TiO<sub>2</sub> material synthesized using the thermal-chemical oxidation of titanium powder (TCO). The study examines the overall confounding effects of the use of methanol when conducting TiO<sub>2</sub> photocatalysis tests on PPCPs.

## 2. Materials and methods

### 2.1. Reagents and chemicals

Titanium powder (~325 mesh, 99.95%), hydrochloric acid (HCl), sodium hydroxide (NaOH), and hydrogen peroxide (H<sub>2</sub>O<sub>2</sub>) were purchased from Sigma-Aldrich while the commercial P25 powder (Aeroxide) was purchased from Evonik Industries. HPLC grade methanol (BDH) was purchased from VWR (Mississauga, ON) while ultrapure water was obtained from a MilliQ water purification system (MilliQ, EMD Millipore, Mississauga, ON). The 15 compounds included in this study have varying solubility and physical-chemical properties (Table 2) and were purchased from Sigma-Aldrich. Their chemical structures are presented in Fig. S4 (Supplementary information). Designated isotopically labeled standards were used for LC–MS/MS

analysis and quantitation (except for monensin) and lorazepam was used as an internal standard (Table S2). These standards were purchased from CDN Isotopes Inc. (Pointe-Claire, QC, Canada), except for atorvastatin-d<sub>5</sub>, which was purchased from Toronto Research Chemicals (Toronto, ON, Canada). The complete list of the deuterated standards employed in this study is provided in Table S2 (Supplementary material). All compounds (regular and deuterated standards) were dissolved in methanol as 1 g/L stock solutions and stored in amber glass vials in a –20 °C freezer.

### 2.2. Thermal-chemical oxidation method (TCO) for nanomaterial synthesis

Titanium powder (1 g) was soaked in 50 mL of 30% H<sub>2</sub>O<sub>2</sub> in a 500-mL clear glass jar which was capped and heat treated for 4 h at 80 °C producing a titanium–titanium dioxide complex in solution. The remaining liquid (yellowish in appearance) was transferred into a second glass jar and dried at 80 °C for 12 h. The powdered material that remained after evaporation was pulverised and heat treated again at 600 °C for 4 h. After the heat treatment, the material was stored in a glass vial and kept in the dark at room temperature.

#### 2.2.1. Nanomaterial characterization

The surface morphology of TiO<sub>2</sub> nanomaterials was characterized by a high resolution transmission electron microscope (HRTEM, JEOL 2010F) at the Canadian Centre for Electron Microscopy (CCEM). TEM samples were prepared by drop casting powder dispersions onto carbon grids. The X-ray photoelectron spectroscopy (XPS) was carried out to verify the presence of TiO<sub>2</sub>. Measurement was conducted using VG Scientific ESCALab 250 system with an aluminum radiation source ( $h\nu = 1486.6$  eV) under ultra-high vacuum. A survey scan was collected at 50 eV pass energy, whereas individual scans (Ti2p and O1s) were collected at 20 eV pass energy. The atomic concentration was calculated using the CasaXPS software (Casa Software Ltd.).

The specific surface area was determined using Brunauer-Emmett-Teller (BET) surface analyzer (Quantachrome Autosorb iQ) using N<sub>2(g)</sub> adsorption data. The band gap of TiO<sub>2</sub> samples was determined by the diffuse reflectance spectra (DRS) using a Shimadzu UV-2501PC UV–vis-NIR spectrophotometer equipped with an integrating sphere accessory, using N<sub>2(g)</sub> as the reference. The details regarding the band gap analysis are described by Hu et al. [22]. A Raman spectrometer (Renishaw RamanScope) equipped with a He-Ne laser (5 mW incident power, 633 nm wavelength) was used to obtain spectra associated with different TiO<sub>2</sub> crystalline phases. Specific information on the TiO<sub>2</sub> Raman mode description is found elsewhere [16].

### 2.3. Experimental setup

Two types of TiO<sub>2</sub> nanomaterials were tested in this study: (1) P25, a commercially available TiO<sub>2</sub> powder and (2) TCO, a powder derived from the thermal-chemical oxidation of titanium powder. Different concentrations of methanol were selected based on the range of values observed in published studies that used methanol as a carrier solvent (Table 1). For each set of experiments, an empty 1 L amber glass solvent bottle was spiked with 200 µL of the 10 mg/L pharmaceutical stock solution in methanol (diluted from 1 g/L solution) and dried at room temperature using N<sub>2(g)</sub>. For P25 experiments, the pharmaceutical compounds were re-solubilized in 1 L ultrapure water and stirred at 1100 rpm for 5 min. Aliquots (300 mL) of this solution containing 2 µg/L of pharmaceuticals were transferred into three beakers for replication were then magnetically stirred (600 rpm) on a four-position stir plate equipped with an in-house designed UV-LED light source casing. Pre-measured P25 powder (30 mg) was added into each beaker and methanol was spiked immediately at different volumes (6, 60, and 600 µL) to obtain 0.002%, 0.02%, and 0.2% of methanol concentration (v/v). The experimental specifications of the photocatalytic batch reactors, including the light intensity, wavelength, and relative distance of the

**Table 2**  
Selected physico-chemical properties of target compounds in this study.

Compound	Abbreviation	Use	Molecular Weight (g/mol)	Log Kow <sup>a</sup>	pKa <sub>1</sub> , pKa <sub>2</sub> , pKa <sub>3</sub> <sup>b</sup>	Solubility in water (at 25 °C, mg/L) <sup>a</sup>
Atenolol	ATEN	Beta-blocker	266.34	−2.5 to 0.31	9.60, 14.08, 15.95	24.24 × 10 <sup>3</sup>
Atorvastatin	ATOR	Lipid lowering	558.64	1.03–4.46	4.33	1.23 × 10 <sup>3</sup>
Atrazine	ATZ	Herbicide	215.68	2.20	1.68	33 (20 °C)
Carbamazepine	CBZ	Anti-epileptic	236.27	1.34–2.5	13.90	18 <sup>c</sup>
Diclofenac	DCF	Anti-inflammatory	296.15	−0.81 to 4.5	4.00	1.13 × 10 <sup>3</sup> (32 °C)
Fluoxetine	FLX	Antidepressant	309.33	0.59–4.65	9.80	50 × 10 <sup>3c</sup>
Gemfibrozil	GEM	Lipid lowering	250.33	1.77–4.4	4.42	125
Ibuprofen	IBU	Anti-inflammatory	206.28	2.97–4.5	4.80	156
Monensin	MON	Antibiotic	692.85	4.82	4.3	NS
Naproxen	NAP	Anti-inflammatory	230.60	3.06–3.22	4.12	15.9
Sulfamethoxazole	SULF	Antibiotic	253.28	−1.54 to 0.95	1.60, 5.70	550 (30 °C)
Triclosan	TCS	Antimicrobial	289.54	3.82–4.8	7.60	11
Triclocarban	TCB	Antimicrobial	315.58	4.71	12.70	2.37 × 10 <sup>−3</sup>
Trimethoprim	TRIM	Antibiotic	290.32	−2.05 to 0.91	7.3	400
Venlafaxine	VEN	Antidepressant	277.40	1.95	8.91, 14.42	267 <sup>c</sup>

Notes: pKa = acid dissociation constant; Kow = octanol-water partition coefficient.

<sup>a</sup> Values were taken from <https://www.reaxys.com> (a range of values were identified to reflect database derived from multiple studies).

<sup>b</sup> pKa was taken from <http://chemicalize.org>.

<sup>c</sup> Value taken from <https://pubchem.ncbi.nlm.nih.gov>; NS = not soluble in water.

LED source to the reactors, are provided elsewhere [16].

An equilibration period of 60 min in the dark was completed prior to exposure to the UV-LED light source. Water samples (5 mL) were collected using a glass pipette into test tubes every 30 min until the exposure reached 210 min. The test tubes were then centrifuged (Sorvall XTR Centrifuge, ThermoFisher) at 3500 rpm for 15 min to separate the TiO<sub>2</sub> particles from the aqueous phase. For TCO powder, 100 mg was initially dispersed for 5 min in 1 L ultrapure water through sonication (Fisherbrand Ultrasonic Cleaner). The solution was transferred to the 1 L amber glass solvent bottle containing the dried pharmaceuticals and the compounds were re-solubilized by stirring for 5 min at 1100 rpm. The same steps for P25 experiments were followed thereafter. All the samples were stored in the dark at 4 °C until sample preparation. Additional control experiments (dark and photolysis experiments, 0% methanol) were also completed. Finally, experiments (n = 3) that determined the formation of hydroxyterephthalic acid (HTPA) upon the reaction of its parent compound (terephthalic acid [TPA]) to hydroxyl radicals were done using the method described in Arlos et al. [23]. This step provided an indication of the photocatalytic activity of the two nanomaterials and the level of hydroxyl radical scavenging by methanol in aqueous solutions.

#### 2.4. Sample preparation and analysis

The samples were spiked with deuterated standard stock solution (final concentration of 20 µg/L) and followed a concentration and purification process via solid phase extraction (SPE) using the same method detailed in Arlos et al. [16]. The analysis of compounds was completed using an Agilent 1200 HPLC (Agilent Technologies) coupled to a mass spectrometer (3200 QTRAP, ABSciex, Concord, ON). The optimized parameter values, including the chromatographic and ionization parameters, data acquisition, and quantitation are also detailed in Arlos et al. [16]. The parameters of additional compounds that were not included in that study are presented in the Supplementary material (Tables S1 and S2). Measured degradation rate constants were fitted using SigmaPlot (Jandel Scientific).

### 3. Results and discussion

#### 3.1. Nanomaterial characterization

The TEM images of the nanomaterials are shown in Fig. 1a. P25 has clustered particles that are 10–30 nm. TCO has micron-sized agglomerated structures that contain crystalline anatase nanorod structures

shown in Fig. 1. The band gap energies of P25 and TCO are 3.05 and 3.00 eV respectively, suggesting that wavelengths below 400 nm are required to create electron-hole pairs (Fig. 2a). The Raman spectra for the materials presented in Fig. 2b show that anatase is the primary crystalline phase for the TCO powder but there are some indications that rutile structures were also produced. The commercially available P25 powder is made up of pure TiO<sub>2</sub> mainly with anatase and rutile content at ~80% and ~20% by weight [24]. The lower bandgap of TCO is due to the higher amount of rutile content in the TCO sample compared to P25. The surface areas of P25 and TCO determined by BET measurements are 57.39 g/m<sup>2</sup> and 27.21 g/m<sup>2</sup> respectively.

XPS spectra were collected and the atomic concentration of Ti and O were determined for P25 and TCO powders as shown in Fig. 3. P25 contained 89.54 at.% of O and 10.46 at.% of Ti, whereas TCO contained 91.05 at.% of O and 8.95 at.% of Ti. The Ti2p<sub>3/2</sub> peak of the TCO spectrum exhibited greater peak broadening than P25 suggesting more surface defects are present in TCO compared to P25 [25].

Based on the physical properties of P25 and TCO, it can be inferred that P25 may be a more effective catalyst than the newly synthesized TCO powder due to high purity TiO<sub>2</sub> content, reported synergetic effect of anatase and rutile configurations found in P25, and relatively higher BET surface area. The mixed crystalline phase of P25 provides hotspots for catalytic reactions, particularly at the anatase-rutile interface [26], and TiO<sub>2</sub> nanomaterials with higher surface area are better photocatalysts due to the availability of more active sites that interact with the target compounds. In addition, the surface defects in TCO contribute to the increased charge carrier recombination which renders the material less active.

#### 3.2. Probing the formation and scavenging of hydroxyl radicals

The probing of the HTPA formation was used as an indirect measurement of the nanomaterial's photocatalytic activity via hydroxyl radical production. HTPA formation at 0% methanol was at least 46 times higher for P25 compared to TCO (Fig. 4, Table S8). P25 was indeed more effective than the newly synthesized TCO. The mixed crystalline phase of P25 provided hotspots for catalytic reactions, particularly at the anatase-rutile interface [26]. Optimization may be required in the future to achieve the potential of TCO powder synthesis for water treatment applications. Nevertheless, it is evident that the presence of methanol impacts the photocatalytic activity of both nanomaterials by scavenging of hydroxyl radicals (i.e. inhibiting HTPA formation) formed during the photo-activation of P25 and TCO (Fig. 4). There was a significant difference in the inhibition of HTPA formation among the

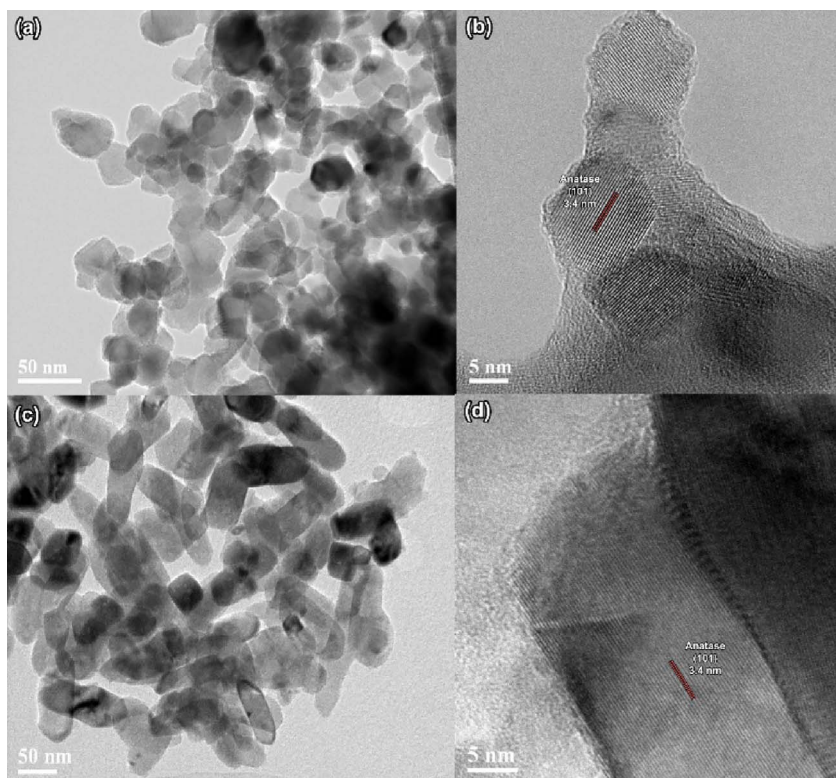


Fig. 1. TEM/HRTEM images of (a and b) P25 and (c and d) TCO powder.

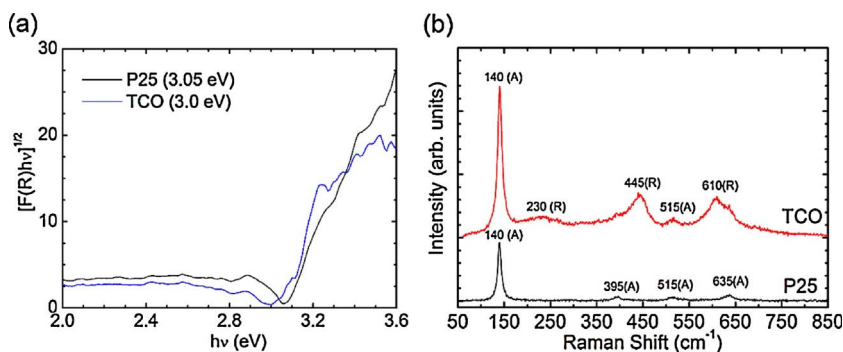


Fig. 2. Additional material characteristics for P25 and TCO powder. (a) band gap energies; (b) Raman spectra.

methanol treatments for both P25 and TCO ( $p < 0.001$ , ANOVA, Tukey Test, post ad-hoc,  $\alpha = 0.05$ ), indicating that even low levels of methanol may be impacting the results of  $\text{TiO}_2$  photocatalytic studies. In particular, adding 0.002% in the experiment reduced the rate of HTPA formation by 20% and 30% for P25 and TCO respectively while 0.2% methanol in the solution inhibits the activity by 98% for both materials.

To gain an improved understanding of the potential mechanisms under the above-mentioned scenarios, the mechanisms of photocatalytic degradation via  $\text{TiO}_2$  need to be carefully examined. When  $\text{TiO}_2$  is activated, electron-hole pairs are generated and the fate of these high-energy charge carriers is dependent on the availability of molecules that can scavenge and/or trap them. Essentially, electrons can be easily scavenged by electron acceptors (e.g. oxygen) producing hydroxyl radicals and/or other ROS while the holes are quenched by electron donors such as water. An organic compound can be degraded directly by the holes or hydroxyl radicals. In circumstances when methanol concentration is low ( $< 0.5 \text{ M}$ ), the oxidation via hydroxyl radical is the likely degradation route [27]. In this study, there is a substantial inhibition of HTPA formation when methanol concentrations in the solutions were increased, likely suggesting that methanol acts as hydroxyl radical scavenger more than a hole scavenger.

### 3.3. Effect of methanol on PPCP photocatalysis

To determine the influence of a carrier solvent during photocatalysis of PPCPs, different amounts of methanol (0%, 0.002%, 0.02%, and 0.2% v/v) were spiked into a solution containing a mixture of target PPCPs and 100 mg/L of  $\text{TiO}_2$  nanomaterials (P25 or TCO). The observed degradation rate constants of most compounds in the presence of UV-LED irradiated P25 were indicative of a pseudo-first order exponential decay:  $C = C_0 e^{-k_p t}$  where  $C_0$  is the initial concentration ( $\mu\text{g/L}$ ),  $t$  is time (min), and  $k_p$  (1/min) is the pseudo first-order decay rate constant (Figs. S1 and S2). The rate constants derived from this equation are shown in Fig. 5 for P25 and Fig. 6 for TCO to illustrate the observed trends (also listed in Tables S3 and S4). The following discussion highlights the potential mechanisms for methanol scavenging of hydroxyl radicals and other ROS and its overall influence in each of the photocatalytic treatment investigation.

#### 3.3.1. P25 experiments

The behavior of the target compounds at different levels of methanol under P25 treatment conditions (Fig. 5) can be categorized into three groups: (1) no effect (Fig. 5a); (2) scavenging effect (Fig. 5b); and, (3) enhanced effect at low levels of methanol (Fig. 5c). The compounds

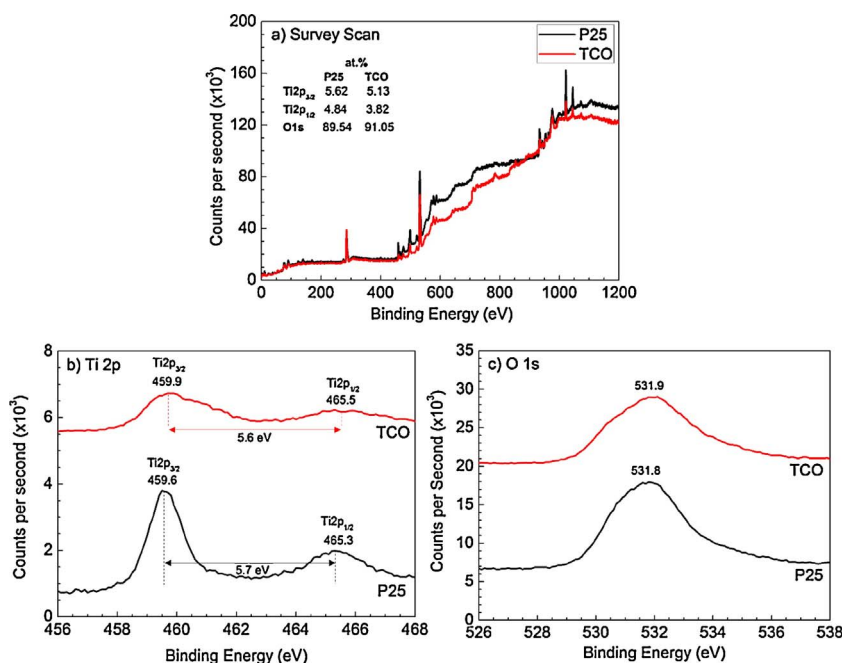


Fig. 3. XPS (a) Survey, (b) Ti2p, (c) O1s scan of P25 and TCO powders.

atorvastatin, atrazine, and naproxen (Fig. 3a) showed statistically similar degradation at all methanol levels (SigmaPlot, One-way ANOVA,  $\alpha = 0.05$ ,  $p = 0.698$  and  $0.089$  respectively). This is a favorable result as these compounds can be introduced in the aqueous solution using methanol (up to 0.2% v/v) without any major consequences. Carbamazepine, diclofenac, fluoxetine, and triclocarban showed reaction inhibition either at 0.002% or 0.02% methanol (Fig. 5b). Above these thresholds, the scavenging effects become evident (see Table S5 of the Supplementary material for  $p$ -values). Hence, it is safe to suggest that methanol may be used to deliver these compounds in the solution during the experiments up to 0.002% or 0.02% v/v.

It appears that for some compounds (atenolol, trimethoprim, venlafaxine, ibuprofen, monensin, and sulfamethoxazole), small amounts of methanol can lead to an enhancement of PPCP degradation (Fig. 5c) but methanol scavenging of hydroxyl radicals or other ROS was still evident at concentrations above these “optimal” conditions (either at 0.002% or 0.02% v/v, Fig. 5c). The rate constants for atenolol, trimethoprim, and venlafaxine at 0.002% methanol were statistically greater than the rate constants observed at 0% methanol ( $p = 0.003$ ,  $0.004$ , and  $0.002$  respectively) but were statistically lower at 0.02% ( $p < 0.001$  for all). A similar pattern was detected for ibuprofen, monensin, and sulfamethoxazole but the “optimal” condition was observed at 0.02% rather than at 0.002%. There appears to be a sporadic pattern for triclosan and gemfibrozil decay rate constants at different methanol concentrations but the highest degradation rate constant was observed at 0.02% and the lowest occurred at 0.2%, when there was the highest amount of methanol in the solution.

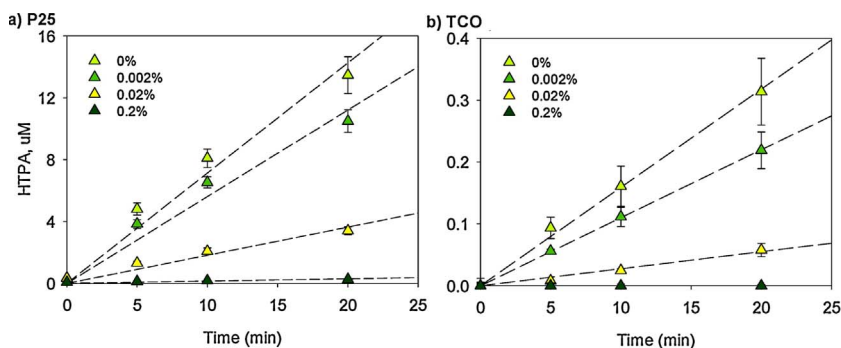


Fig. 4. HTPA formation for (a) P25 and (b) TCO at different concentrations of methanol. The average rates of HTPA formation are found in the Supplementary material (Table S8).

The dark control experiments conducted without methanol showed no significant loss of compounds via adsorption onto  $\text{TiO}_2$  or glass walls (except for atorvastatin and monensin, Fig. S3). The results for photolysis experiments (UV-LED only) were also similar, with only three compounds (atorvastatin, monensin, and triclocarban) showing susceptibility to degradation after UV-LED irradiation only (Fig. S3). Note that improvements in the photocatalytic degradation behavior were observed for those compounds that were prone to both adsorption (dark control) and photolysis (UV-LED exposure only).

The results showing that some compounds (atorvastatin, atrazine, and naproxen) were not affected by methanol at any of the methanol concentrations evaluated under P25 treatment suggest that either these compounds have (1) better reactivity towards P25 than methanol or (2) undergo a degradation pathway (e.g., via SET mechanism) that is not exacerbated by methanol. Other factors such as exposure to UV-LED alone or adsorption onto  $\text{TiO}_2$  may play a role for the non-observable effects of methanol on their degradation. This process is primarily illustrated by atorvastatin, a compound which is susceptible to both  $\text{TiO}_2$  adsorption and photolysis reactions (Fig. S3). By contrast, compounds that have been affected by methanol may have competed with the carrier solvent for reaction sites on  $\text{TiO}_2$  surfaces and/or hydroxyl radicals generated after the photo-activation.

Some studies have suggested that the presence of scavengers (radical, electron, or hole scavengers) can enhance photocatalysis by preventing the recombination of charge carriers [28] or by producing highly reactive by-products that can additionally “attack” the target compounds (e.g. photosensitizers) [29,30]. A previous work on the

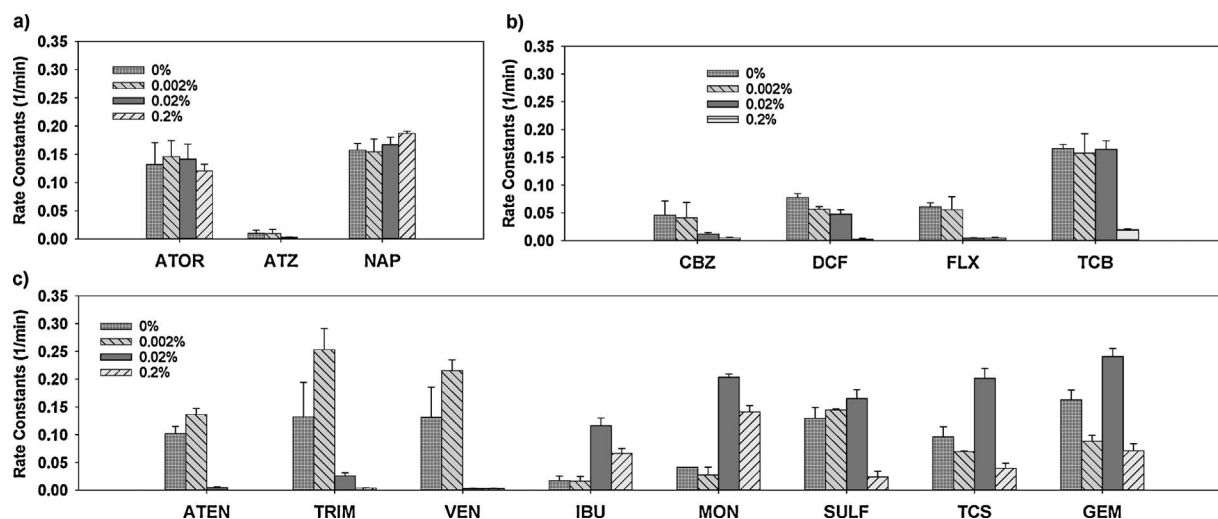


Fig. 5. Pseudo first-order rate constants for all target compounds using UV-LED irradiated P25 powder at different methanol concentrations. a) Compounds that were not affected by the presence of methanol. b) Compounds with rate constants decreasing at increasing methanol concentration. c) Compounds with rate constants enhanced by some levels of methanol in the solution.

photocatalytic decomposition of polycyclic aromatic hydrocarbons (PAHs) further indicated an efficient degradation due to the enhanced solubility of PAHs under the presence of a carrier solvent (acetone) [18]. Zhu et al. [31] observed an improvement in the photocatalytic degradation of pyridaben (pesticide, water solubility of  $1.2 \times 10^{-2}$  mg/L, 25 °C) when the amounts of acetone were slightly increased. Skaf et al. [19] also found a similar result when 1,3-dinitrobenzene, a compound with comparable solubility to our target chemicals (533 mg/L, 25 °C), was introduced to the solution with a carrier solvent during TiO<sub>2</sub> photocatalysis. We recognize that additional studies are needed to confirm these results (especially for gemfibrozil and triclosan) and to identify the fundamental mechanisms of photocatalytic enhancement by scavengers.

### 3.3.2. TCO experiments

Unlike the variable behavior of target compounds under P25 treatments, the rate constants calculated for TCO treatments showed a decreasing trend, as the concentrations of methanol in solution increased (Fig. 6). This observation demonstrates the “classic” scavenging effect of methanol during TiO<sub>2</sub> photocatalysis as per the inhibition of HTPA formation shown earlier (Fig. 4). A significant difference was detected even when the methanol concentration was added at the lowest level evaluated in the study (0.002% v/v) for some compounds, especially atorvastatin, diclofenac, and naproxen. Other compounds, in contrast, showed a significant drop in the first order kinetic rate

constants when methanol was at 0.02% or 0.2% v/v (*p*-values are presented in Table S6). A few compounds (atrazine, carbamazepine, ibuprofen, and venlafaxine) showed no degradation during the irradiation period, even without methanol. For TCO, it may be better to eliminate the use of a carrier solvent such as methanol as the scavenging effect was very pronounced even at low levels of methanol.

Additional studies could be done in the future to understand the differences in the results observed for P25 and TCO. For example, application of structure-activity relationships (SAR) for hydroxyl radical reactions could help clarify the patterns detected (e.g. why certain compounds have higher reactivity towards P25). It is clear in this present study that the use of carrier solvent has consequences for future experimental design and the interpretation of the results. For example, the use of excess methanol may confound the subsequent comparisons among new materials or among different water sources/quality.

### 3.3.3. Implications of the use of methanol for designing treatment experiments

The varying behavior of PPCPs under the presence of a carrier solvent, such as methanol as outlined above, has consequences in the design of experiments that evaluate the photocatalytic degradation of organic compounds in mixtures. When it comes to comparing the reaction or treatment efficiency of two or more nanomaterials, it is intuitively important to complete the experiments under the same conditions (e.g. same methanol concentration all throughout). However, as

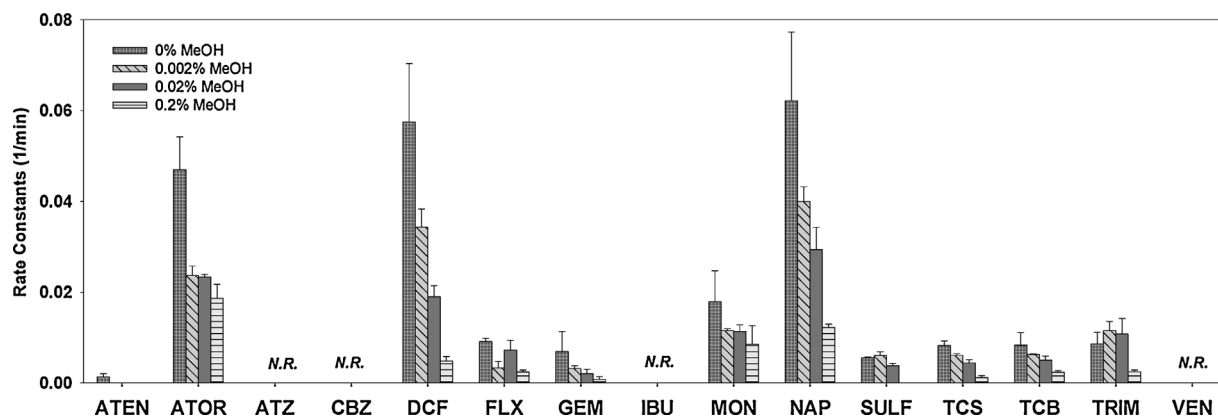


Fig. 6. Pseudo first-order rate constants for all target compounds using UV-LED irradiated TCO powder. Pseudo first-order rate constants for all compounds decreased with increasing methanol concentration. N.R. = no response in the treatment.

was demonstrated in this study, not all TiO<sub>2</sub> nanomaterials (or chemicals) behave similarly in the presence of methanol as a carrier solvent (i.e. scavenging effect in TCO, but not necessarily for P25). It appears that materials with lower reactivity such as TCO are easier targets for methanol scavenging. An investigator without *a priori* knowledge on the treatment efficiency of a new catalyst may conduct the experiments at different starting points (e.g. deliver target compounds using a carrier solvent at a relatively higher concentration). This is particularly important for investigators that are optimizing new materials, as future results may be misinterpreted.

Early investigations on the degradation of organic compounds in aqueous solutions using TiO<sub>2</sub> did not require the use of carrier solvents such as methanol because the model chemicals being investigated were very soluble in water (e.g. dye, organic acids, or phenolic compounds such as 4-chlorophenol). However, efforts to examine the use of TiO<sub>2</sub> for water treatment applications have expanded beyond the use of these highly water-soluble chemicals because they are not necessarily representative of the compounds being addressed by water treatment systems currently. Investigations have now included very diverse groups of compounds with varying types and levels of physical and chemical properties, including water solubility. While it may be more beneficial to conduct experiments without the use of a carrier solvent such as methanol, caution must be undertaken if it is used.

Westerhoff et al. [32] suggested the use of acetone to introduce the pharmaceuticals in aqueous solutions instead of methanol as the radical scavenging effect is not as pronounced. Other organic solvents may also be used but recognizing the pathway they scavenge is beneficial for the interpretation of the experimental results. For instance, dimethylsulfoxide (DMSO) is a commonly used carrier solvent but is also known to scavenge electrons. If the degradation pathway of the target compound (s) is via SET, then DMSO may not impact the overall photocatalytic process. Regardless of the direction chosen, investigators must carefully assess the influence of the carrier solvent in the overall photocatalytic degradation and, at the very least, explicitly report its use during the experiment.

#### 4. Conclusions

The use of a carrier solvent to deliver PPCPs and other similar compounds into aqueous solutions is a common practice used for preparing solutions for radical-mediated degradation experiments using photocatalytic materials such as TiO<sub>2</sub>. However, the presence of a carrier solvent such as methanol can greatly reduce the chemical degradation rates during TiO<sub>2</sub> photocatalysis due to its inherent scavenging effect. In this study, we examined four levels of methanol concentrations that are representative of what has been used in the literature: 0%, 0.002%, 0.02% and 0.2% v/v methanol. The lowest level, 0.002% v/v, did not influence the rates of photocatalytic degradation of some target compounds when treated with a more photoactive TiO<sub>2</sub> nanomaterial such as P25. This result suggests that future studies using P25 alone may be able to use trace amounts of methanol as a carrier but higher levels may confound the results. However, the influence of methanol when using a less reactive material such as the newly synthesized material included in this study (i.e. TiO<sub>2</sub> produced under thermal-chemical oxidation of titanium powder) was more pronounced than when using P25. It would be ideal to conduct experiments without a solvent carrier as even as little as 0.002% v/v methanol had some confounding effects. The results of this study illustrate that the effect of methanol as a carrier solvent must be assessed in radical-mediated testing especially for comparisons of newly synthesized TiO<sub>2</sub> nanomaterials (e.g. TCO) to avoid unbiased interpretation of experimental results.

#### Acknowledgments

This work was funded through Natural Sciences and Engineering

Research Council (NSERC) of Canada – Strategic Project Grant (STPGP 430654-12). We would like to acknowledge the help and assistance provided by the Servos Lab Group – Department of Biology, Schwartz-Reisman Foundation, Waterloo-Technion Research Co-operation Program, and Centre of Advanced Materials Joining at the University of Waterloo.

#### Appendix A. Supplementary data

Supplementary data associated with this article can be found, in the online version, at <http://dx.doi.org/10.1016/j.jece.2017.08.048>.

#### References

- [1] A. Fujishima, K. Honda, Electrochemical hotolysis of water at a semiconductor electrode, *Nature* 238 (1972) 37–38.
- [2] A.R. Khataee, M.B. Kasiri, Photocatalytic degradation of organic dyes in the presence of nanostructured titanium dioxide: influence of the chemical structure of dyes, *J. Mol. Catal. A: Chem.* 328 (2010) 8–26.
- [3] K. Hashimoto, H. Irie, A. Fujishima, TiO<sub>2</sub> photocatalysis: a historical overview and future prospects, *Jpn. J. Appl. Phys.* 44 (2005) 8269.
- [4] M.N. Chong, B. Jin, C.W. Chow, C. Saint, Recent developments in photocatalytic water treatment technology: a review, *Water Res.* 44 (2010) 2997–3027.
- [5] L.J. Schimmoller, M.J. Kealy, S.K. Foster, Triple bottom line costs for multiple potable reuse treatment schemes, *Environ. Sci.: Water Res. Technol.* 1 (2015) 644–658.
- [6] C.G. Daughton, T.A. Ternes, Pharmaceuticals and personal care products in the environment: agents of subtle change? *Environ. Health Perspect.* 107 (1999) 907.
- [7] A.C. Tong, R. Braund, D. Warren, B. Peake, TiO<sub>2</sub>-assisted photodegradation of pharmaceuticals—a review, *Cent. Eur. J. Chem.* 10 (2012) 989–1027.
- [8] N. Miranda-García, S. Suárez, B. Sánchez, J.M. Coronado, S. Malato, M.I. Maldonado, Photocatalytic degradation of emerging contaminants in municipal wastewater treatment plant effluents using immobilized TiO<sub>2</sub> in a solar pilot plant, *Appl. Catal. B* 103 (2011) 294–301.
- [9] N. Miranda-García, M.I. Maldonado, J.M. Coronado, S. Malato, Degradation study of 15 emerging contaminants at low concentration by immobilized TiO<sub>2</sub> in a pilot plant, *Catal. Today* 151 (2010) 107–113.
- [10] Y. Nosaka, A.Y. Nosaka, Identification and roles of the active species generated on various photocatalysts, in: P. Pichat (Ed.), *Photocatalysis and Water Purification: From Fundamentals to Recent Applications*, Wiley-VCH Verlag GmbH & Co. KGaA, Weinham, Germany, 2013, pp. 3–24.
- [11] T. Paul, P.L. Miller, T.J. Strathmann, Visible-light-mediated TiO<sub>2</sub> photocatalysis of fluoroquinolone antibacterial agents, *Environ. Sci. Technol.* 41 (2007) 4720–4727.
- [12] W.S. Jenks, Photocatalytic reaction pathways-effects of molecular structure, catalyst, and wavelength, in: P. Pichat (Ed.), *Photocatalysis and Water Purification: From Fundamentals to Recent Applications*, Wiley-VCH, Weinham, Germany, 2013pp. 25–51.
- [13] D.A. Panayotov, S.P. Burrows, J.R. Morris, Photooxidation mechanism of methanol on rutile TiO<sub>2</sub> nanoparticles, *J. Phys. Chem. C* 116 (2012) 6623–6635.
- [14] Y. Sun, J.J. Pignatello, Evidence for a surface dual hole-radical mechanism in the titanium dioxide photocatalytic oxidation of 2,4-D, *Environ. Sci. Technol.* 29 (1995) 2065–2072.
- [15] R. Molinari, C. Lavorato, P. Argurio, Photocatalytic reduction of acetophenone in membrane reactors under UV and visible light using TiO<sub>2</sub> and Pd/TiO<sub>2</sub> catalysts, *Chem. Eng. J.* 274 (2015) 307–316.
- [16] M.J. Arlos, M.M. Hatat-Fraile, R. Liang, L.M. Bragg, N.Y. Zhou, S.A. Andrews, M.R. Servos, Photocatalytic decomposition of organic micropollutants using immobilized TiO<sub>2</sub> having different isoelectric points, *Water Res.* 101 (2016) 351–361.
- [17] W. Sun, S. Li, J. Mai, J. Ni, Initial photocatalytic degradation intermediates/pathways of 17 $\alpha$ -ethynylestradiol: effect of pH and methanol, *Chemosphere* 81 (2010) 92–99.
- [18] O.T. Woo, W.K. Chung, K.H. Wong, A.T. Chow, P.K. Wong, Photocatalytic oxidation of polycyclic aromatic hydrocarbons: intermediates identification and toxicity testing, *J. Hazard. Mater.* 168 (2009) 1192–1199.
- [19] D. Skaf, A. Grannas, D. Colotti, E. Bowes, The effects of photocatalyst and solution co-contaminants on photocatalytic oxidation of 1,3-dinitrobenzene in aqueous semiconductor oxide suspensions, *J. Chem. Eng. Process Technol.* 7 (2016) 1–6.
- [20] A. Nikolaou, S. Meric, D. Fatta, Occurrence patterns of pharmaceuticals in water and wastewater environments, *Anal. Bioanal. Chem.* 387 (2007) 1225–1234.
- [21] B. Kasprzyk-Hordern, R.M. Dinsdale, A.J. Guwy, The removal of pharmaceuticals personal care products, endocrine disruptors and illicit drugs during wastewater treatment and its impact on the quality of receiving waters, *Water Res.* 43 (2009) 363–380.
- [22] A. Hu, X. Zhang, K.D. Oakes, P. Peng, Y.N. Zhou, M.R. Servos, Hydrothermal growth of free standing TiO<sub>2</sub> nanowire membranes for photocatalytic degradation of pharmaceuticals, *J. Hazard. Mater.* 189 (2011) 278–285.
- [23] M.J. Arlos, R. Liang, M.M. Hatat-Fraile, L.M. Bragg, N.Y. Zhou, M.R. Servos, S.A. Andrews, Photocatalytic decomposition of selected estrogens and their estrogenic activity by UV-LED irradiated TiO<sub>2</sub> immobilized on porous titanium sheets via thermal-chemical oxidation, *J. Hazard. Mater.* 318 (2016) 541–550.
- [24] Evonik, AEROXIDE<sup>®</sup>, AERODISP<sup>®</sup> and AEROPERL<sup>®</sup> Titanium Dioxide as

- Photocatalyst: Technical Information 1243, in, 2015.
- [25] W. Göpel, J. Anderson, D. Frankel, M. Jaehning, K. Phillips, J. Schäfer, G. Rocker, Surface defects of TiO<sub>2</sub> (110): a combined XPS, XAES and ELS study, *Surf. Sci.* 139 (1984) 333–346.
- [26] D.C. Hurum, A.G. Agrios, K.A. Gray, T. Rajh, M.C. Thurnauer, Explaining the enhanced photocatalytic activity of Degussa P25 mixed-phase TiO<sub>2</sub> using EPR, *J. Phys. Chem. B* 107 (2003) 4545–4549.
- [27] L. Sun, J.R. Bolton, Determination of the quantum yield for the photochemical generation of hydroxyl radicals in TiO<sub>2</sub> suspensions, *J. Phys. Chem.* 100 (1996) 4127–4134.
- [28] A. Syoufian, K. Nakashima, Degradation of methylene blue in aqueous dispersion of hollow titania photocatalyst: study of reaction enhancement by various electron scavengers, *J. Colloid Interface Sci.* 317 (2008) 507–512.
- [29] S. Rengaraj, X.Z. Li, Enhanced photocatalytic reduction reaction over Bi<sup>3+</sup> + -TiO<sub>2</sub> nanoparticles in presence of formic acid as a hole scavenger, *Chemosphere* 66 (2007) 930–938.
- [30] X. Zhu, D. Zhou, L. Cang, Y. Wang, TiO<sub>2</sub> photocatalytic degradation of 4-chlorobiphenyl as affected by solvents and surfactants, *J. Soils Sediments* 12 (2012) 376–385.
- [31] X. Zhu, C. Yuan, Y. Bao, J. Yang, Y. Wu, Photocatalytic degradation of pesticide pyridaben on TiO<sub>2</sub> particles, *J. Mol. Catal. A: Chem.* 229 (2005) 95–105.
- [32] P. Westerhoff, Y. Yoon, S. Snyder, E. Wert, Fate of endocrine-disruptor, pharmaceutical, and personal care product chemicals during simulated drinking water treatment processes, *Environ. Sci. Technol.* 39 (2005) 6649–6663.
- [33] G. Li Puma, V. Puddu, H.K. Tsang, A. Gora, B. Toepfer, Photocatalytic oxidation of multicomponent mixtures of estrogens (estrone (E1), 17β-estradiol (E2), 17α-ethynylestradiol (EE2) and estriol (E3)) under UVA and UVC radiation: photon absorption, quantum yields and rate constants independent of photon absorption, *Appl. Catal. B: Environ.* 99 (2010) 388–397.
- [34] D. Nasuhoglu, D. Berk, V. Yargeau, Photocatalytic removal of 17α-ethynylestradiol (EE2) and levonorgestrel (LNG) from contraceptive pill manufacturing plant wastewater under UVC radiation, *Chem. Eng. J.* 185–186 (2012) 52–60.
- [35] R. Kralchevska, M. Milanova, M. Bistan, A. Pintar, D. Todorovsky, The photocatalytic degradation of 17α-ethynylestradiol by pure and carbon nanotubes modified TiO<sub>2</sub> under UVC illumination, *Cent. Eur. J. Chem.* 10 (2012) 1137–1148.
- [36] B.A. Marinho, M.V. de Liz, E.R. Lopes Tiburtius, N. Nagata, P. Peralta-Zamora, TiO<sub>2</sub> and ZnO mediated photocatalytic degradation of E2 and EE2 estrogens, *Photochem. Photobiol. Sci.* 12 (2013) 678–683.
- [37] R.L. Fernández, J.A. McDonald, S.J. Khan, P. Le-Clech, Removal of pharmaceuticals and endocrine disrupting chemicals by a submerged membrane photocatalysis reactor (mpr), *Sep. Purif. Technol.* 127 (2014) 131–139.
- [38] N. Miranda-García, S. Suárez, M.I. Maldonado, S. Malato, B. Sánchez, Regeneration approaches for TiO<sub>2</sub> immobilized photocatalyst used in the elimination of emerging contaminants in water, *Catal. Today* 230 (2014) 27–34.
- [39] Y. Yang, L. Luo, M. Xiao, H. Li, X. Pan, F. Jiang, One-step hydrothermal synthesis of surface fluorinated TiO<sub>2</sub>/reduced graphene oxide nanocomposites for photocatalytic degradation of estrogens, *Mater. Sci. Semicond. Process.* 40 (2015) 183–193.
- [40] J. Colina-Márquez, F. Machuca-Martínez, G. Li Puma, Modeling the photocatalytic mineralization in water of commercial formulation of estrogens 17-β estradiol (E2) and norgestrel acetate in contraceptive pills in a solar powered compound parabolic collector, *Molecules* 20 (2015) 13354–13373.